Basin bifurcations in quasiperiodically forced coupled systems

Manish Dev Shrimali,[1,2] Awadhesh Prasad,[3] Ram Ramaswamy,[2,4] and Ulrike Feudel[5]
[1]*Department of Physics, Dayanand College, Ajmer 305 001, India*
[2]*School of Physical Sciences, Jawaharlal Nehru University, New Delhi 110 067, India*
[3]*Department of Physics and Astrophysics, Delhi University, Delhi, 110 007, India*
[4]*School of Natural Sciences, Institute for Advanced Study, Princeton NJ 08540, USA*
[5]*Institute for Chemistry and Biology of the Marine Environment, University of Oldenburg, PF 2503, D-26111 Oldenburg, Germany*
(Received 1 December 2004; published 22 September 2005)

We study the effect of quasiperiodic forcing on a system of coupled identical logistic maps. Upon a variation of system parameters, a variety of different dynamical regimes can be observed, including phenomena such as bistability and multistability. At the bifurcation to bistability, in a manner reminiscent of attractor expansion at interior crises, there is an abrupt change in the size of attractor basins. In the bistable region, attractor basins undergo additional bifurcations wherein holes and islands are created within the basins when system parameters change. These can be understood by examining critical surfaces for the coupled system.

DOI: 10.1103/PhysRevE.72.036215 PACS number(s): 05.45.Xt

I. INTRODUCTION

The dynamics of coupled nonlinear systems has attracted much interest in the past decades in many areas of science. Such systems have been modeled by coupled ordinary differential equations or through coupled map lattices [1]. A number of interesting complex dynamical phenomena that have been theoretically and experimentally revealed in investigations [2–4] include antiphase states, spatiotemporal intermittency, attractor crowding, turbulence, traveling waves, and synchronization.

In this paper we consider the influence of external driving by a force that is *quasiperiodic* in time on coupled nonlinear systems. Such forcing has been extensively studied in the past few years for a variety of reasons, including the fact that with quasiperiodic driving, the dynamics can be both aperiodic and stable, when confined to so-called strange nonchaotic attractors (SNAs) [5,6]. These attractors possess only nonpositive Lyapunov exponents (LEs) and are hence nonchaotic, and they are also typically geometrically fractal (hence strange).

We examine the simplest case, where two coupled systems are driven by a common quasiperiodic force. The model we study in some detail consists of coupled logistic maps, a system whose behavior, both in the absence of driving [7,8] as well as in the absence of coupling [5,9,10] has been extensively studied in the past. This permits a clearer identification of new features of the dynamics in the coupled and forced system. Uncoupled logistic maps individually follow the period-doubling route to chaos, while in general, it is known that quasiperiodic forcing transforms periodic attractors to quasiperiodic ones, truncates the period-doubling cascade, and makes a transition to SNA possible [5,11,12].

A striking phenomenon that can be observed in coupled systems is synchronization [13]. Even when the dynamics is chaotic, namely showing sensitivity to initial conditions, Pecora and Carroll [14] showed that identical (or nearly identical) nonlinear systems can be synchronized if coupled through a common drive signal. The motion of the coupled system eventually (i.e., after transient unsynchronized dynamics) takes place on an attractor that is contained in a lower-dimensional subspace of the entire phase space: this is the "synchronization manifold" [15]. The synchronization manifold is an invariant symmetric subspace (ISS), and the stability of synchronization can be measured through the transverse Lyapunov exponent [8,16].

Identical quasiperiodically driven uncoupled systems synchronize on SNAs [17]. When the coupled system is driven quasiperiodically, synchronization becomes possible under three separate scenarios: the attractor in the invariant subspace can be (i) chaotic and strange, (ii) nonchaotic and strange, or (iii) nonchaotic and nonstrange. Furthermore, and similar to the unforced case [7,8], there are a number of bifurcations and transitions both in the dynamics as well as in the nature of the attractor basins.

Very recently, Neumann, Sushko, Maistrenko, and Feudel [18] have studied a related coupled logistic map system with additive quasiperiodic driving. While the effect of additive forcing is similar to multiplicative driving that we employ, the focus of their study is on the synchronization behavior, and thus it is somewhat different from that of the present work, which examines the basins of attraction of coexisting attractors. Nevertheless, the two studies are complementary, and provide a fairly detailed view of quasiperiodically driven coupled logistic maps. Coexisting synchronized as well as nonsynchronized SNAs have also been studied in a different system of coupled quasiperiodically forced logistic maps [19].

Multistability—the coexistence of two or more attractors with separate basins of attraction in phase space—is typical in nonlinear dynamical systems [20–22]. As a control parameter varies, attractors may appear, disappear, or change stability through different bifurcations. In some cases the bifurcations of attractors are accompanied by transformations of their basins of attractions so that their structure may be very complicated, or even fractal. In the present work we study in detail the bifurcations leading to bistability in driven coupled logistic maps, and describe the basin boundary bifurcations in the region of bistability.

The coupled system we study here is described in the following section. Since there are several parameters in the model, we restrict our analysis to a typical region in the parameter space and discuss the different dynamical regimes that occur. When the control parameter varies there is a sequence of bifurcations, both within the ISS as well as outside it. These give rise to different stability regions, including the region of bistability with coexisting synchronous and asynchronous attractors. These phenomena are discussed in Sec. III for particular but representative values of the system parameters. The size of the basin of the synchronized attractor is seen to undergo an abrupt increase at a particular parameter value: this feature is similar, both qualitatively and quantitatively, to the dynamical behavior at an interior crisis [23]. A basin boundary bifurcation occurs in the forced coupled system in the bistability region and this can be understood through an extension of the theory of critical curves [24] presented in Sec. IV. We conclude this paper with a discussion and summary in Sec. V.

II. SYSTEM AND DYNAMICS

Consider two symmetrically coupled identical logistic maps, both subject to a common quasiperiodic parametric modulation,

$$x_{n+1} = \alpha[1 + \epsilon \cos(2\pi\theta_n)]x_n(1 - x_n) + \beta(y_n - x_n),$$

$$y_{n+1} = \alpha[1 + \epsilon \cos(2\pi\theta_n)]y_n(1 - y_n) + \beta(x_n - y_n),$$

$$\theta_{n+1} = \theta_n + \omega, \quad \mod 1. \tag{1}$$

The variables of the two maps are denoted by x and y for clarity. We retain the skew-product structure of earlier studies [5] of quasiperiodically driven systems; the θ dynamics is a rigid irrational rotation, unaffected by the variation of the other variables. The driving frequency is an irrational number, the inverse of the golden mean ratio, $\omega=(\sqrt{5}-1)/2$. Parameters for the maps governing evolution of the variables x and y have been taken to be identical for convenience, and the coupling is symmetric.

The phase space of the three-dimensional system is $I^2 \times S^1$, I being the unit interval. The dynamics (1) leaves the phase space invariant in the absence of coupling (i.e., $\beta=0$). For $\epsilon \neq 0$, it is clear that the motion will remain bounded in this region as long as $\alpha[1+\epsilon\cos(2\pi\theta_n)] \in [0, 4]$. Thus for any $\alpha \leqslant 4$, the largest allowed value of ϵ is $4/\alpha-1$. The driving parameter is rescaled as $\epsilon' = \epsilon/(4/\alpha-1)$ and we study the system for $0 \leqslant \epsilon' \leqslant 1$. The main bifurcation parameter is α.

Since the dynamics of the θ variable is uniform and ergodic, it is convenient to consider the reduced phase space spanned by the variables x and y. The synchronization manifold, the plane $\{x=y, \theta\}$, is invariant: a trajectory with initial conditions in this manifold subsequently remains within the manifold. Further, since the coupling term vanishes, synchronized dynamics is effectively described by the single forced logistic map,

$$x_{n+1} = f(x_n, \theta_n) = \alpha[1 + \epsilon \cos(2\pi\theta_n)]x_n(1 - x_n),$$

$$y_{n+1} = x_{n+1},$$

$$\theta_{n+1} = \theta_n + \omega, \quad \mod 1. \tag{2}$$

The within-ISS Lyapunov exponent is

$$\lambda = \lim_{N\to\infty} \frac{1}{N} \sum_{i=1}^{N} \ln|f'(x_i, \theta_i)|, \tag{3}$$

while in the direction transverse to the synchronization manifold, the transverse LE is

$$\lambda_\perp = \lim_{N\to\infty} \frac{1}{N} \sum_{i=1}^{N} \ln|f'(x_i, \theta_i) - 2\beta|. \tag{4}$$

Regions in parameter space where the transverse Lyapunov exponent $\lambda_\perp$ is negative are characterized by synchronization with the attractor in the ISS being stable (or at least weakly stable [25]). Upon variation of system parameters, synchronization can be lost via a blowout bifurcation [18,26] if the transverse LE becomes positive.

The case $\beta=0$, namely the (single) quasiperiodically forced logistic map has been studied extensively in the context of strange nonchaotic attractors [5,9,10]. In the absence of quasiperiodic forcing, i.e. for $\epsilon'=0$, the logistic map displays a period-doubling cascade to chaos as the bifurcation parameter α is varied [27]. With quasiperiodic driving the periodic attractors of the logistic map become quasiperiodic attractors: period-n orbits of the logistic map are converted into tori with n branches. Besides the usual chaotic attractors, strange nonchaotic attractors exist in the forced system. In general, quasiperiodic forcing suppresses the infinite cascade of period-doubling bifurcations; only a finite number of torus doublings occur and these are often shifted to larger values of the parameter [10]. Strange nonchaotic dynamics typically occurs in the transition from quasiperiodic torus attractors to chaotic attractors [5].

The case of coupled logistic maps without external forcing, namely $\beta \neq 0$, $\epsilon'=0$ has been studied extensively [7,8]. This coupled system exhibits multistability, namely the coexistence of numerous attractors in phase space. The basin of attraction of the synchronized attractor in the ISS can undergo the so-called riddling bifurcation [8] when the attractor itself becomes weakly stable.

The phase diagram in the α, ϵ' parameter plane is shown in Fig. 1 for $\beta=0.01$. A variety of dynamical behaviors can be observed upon variation of the parameters α, β, and ϵ, and the cases depicted in Fig. 1 (see the caption) are typical. The different regions of stability are indicated via shading: the region where only the synchronized attractor exists is shown in dark gray, while the region where both synchronized and nonsynchronized attractors coexist (namely bistability) is shown in light gray. There is a loss of stability of the ISS attractor in a blowout bifurcation at the right boundary of the dark gray region. In the unshaded region, the attractor outside the ISS is asynchronous. The transition to bistability, shown by a dark line on the left boundary of the light gray region, is marked by the coexistence of the synchronous attractor in the ISS with the asynchronous attractor outside the ISS. There are small regions where only the syn-

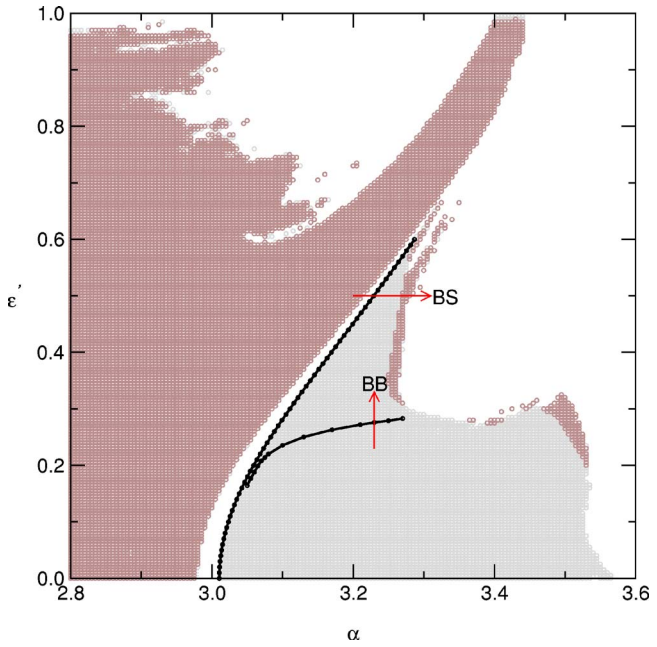

FIG. 1. (Color online) Partial phase diagram in the α ,ϵ' parameter plane for β=0.01. The region of complete synchronization is shown in dark gray and the region of multistability in light gray. The white region corresponds to $\lambda_\perp > 0$. The subcritical pitchfork bifurcation leading to bistability is shown by a line at the boundary of light gray region and the transition to bistability is marked as BS. The basin bifurcation line is shown in the bistability region and the transition is marked BB.

chronous attractor exists within the ISS occur at the boundaries of the light gray region on the other side.

III. TRANSITIONS TO MULTISTABILITY

In this section we examine mechanisms of the occurrence of multistability, namely the coexistence of two or more attractors for a fixed set of parameters [28,29]. We also investigate the evolution of the corresponding attractor basins, the set of all initial conditions that converge to it asymptotically under the dynamics. The basins are numerically computed, starting with a grid of $10^3 \times 10^3$ different initial conditions in the $x-y$ plane and iterating for a sufficiently long time (here 10^5 iterations). For most of the parameter values studied here we observe coexisting attractors: one in the ISS and one (or, rarely, more) outside the ISS. When there is only the attractor in the ISS, i.e., only a synchronized state exists, then it is also a global attractor: all points in the phase space are attracted to it.

We first discuss and review the bifurcations in the unforced case of Eq. (1) with $\epsilon'=0$ [30,31]. The coupled system is invariant under the exchange of variables and therefore the system has either symmetric or nonsymmetric solutions. The symmetric solutions of the coupled system are the solutions of the logistic map because the coupling term then vanishes.

The symmetric fixed point (x_f, x_f) of the coupled system is given by

$$x_f = \frac{\alpha - 1}{\alpha}. \tag{5}$$

The stability of a period-p orbit of the coupled system will be determined by the eigenvalues of the Jacobian matrix,

$$J = \prod_{n=1}^{p} \begin{bmatrix} f'(x_n) - \beta & \beta \\ \beta & f'(x_n) - \beta \end{bmatrix}.$$

For the symmetric fixed point x_f (Eq. (5)) the eigenvalues are

$$\eta_1 = 2 - \alpha \text{ and } \eta_2 = 2 - \alpha - 2\beta. \tag{6}$$

There are two period-doubling bifurcations in the coupled system, and these give rise to unstable symmetric and stable asymmetric period-2 orbits at $\alpha=3$ and $\alpha=3-2\beta$, respectively. The symmetric period-2 orbit is (x_1^s, x_1^s), (x_2^s, x_2^s), where

$$x_{1,2}^s = a \pm \sqrt{b}, \tag{7}$$

with

$$a = \frac{\alpha + 1}{2\alpha} \quad \text{and} \quad b^2 = \frac{(\alpha - 1)^2 - 4}{4\alpha^2}. \tag{8}$$

The eigenvalues of the symmetric period-2 orbit (see Eq. (7)) are

$$\eta_1 = 5 - (\alpha - 1)^2 \quad \text{and} \quad \eta_2 = 5 - (\alpha - 1)^2 + 4\beta(\beta + 1). \tag{9}$$

The symmetric period-2 orbit that appears at $\alpha=3$ is unstable and changes stability in a subcritical pitchfork bifurcation at

$$\alpha = 1 + 2(1 + \beta + \beta^2)^{1/2}. \tag{10}$$

The stable symmetric period-2 orbit loses stability again in another period-doubling bifurcation at $\alpha=1+\sqrt{6}$. The assymmetric period-2 orbit (x_1^a, y_1^a), (x_2^a, y_2^a) that appears at $\alpha=3-2\beta$ is stable before it undergoes a Hopf bifurcation. Hence there are regions in the coupled system where there are two or more coexisting attractors, depending on the values of the control parameters. These different regions of stability of the unforced coupled map system are located along the $\epsilon'=0$ line in Fig. 1.

For $\epsilon'=0.5$ at $\beta=0.01$, corresponding to the arrow denoted by *BS* in the phase diagram, Fig. 1, there are regions with synchronization only (dark gray) or regions with coexisting attractors (light gray) depending on the nonlinearity, and the nonzero LEs for the system, Eqs. (1), are shown in Fig. 2(a) as a function of the parameter α. The transverse Lyapunov exponent and the Lyapunov exponent in the ISS are given in Fig. 2(b). Since there can be coexisting attractors in the system, we compute the spectrum of LEs as follows. Starting with initial conditions of x and θ fixed at 0.5 and 0, respectively, a number of different initial y's are sampled in the interval [0, 1]. Since the system has three LEs for a given initial y, there can either be two distinct nonzero LEs if there is a single attractor, or n pairs of distinct nonzero LEs when there are n distinct attractors. (The irrational rotation in θ always gives a zero LE). Therefore in the bistability

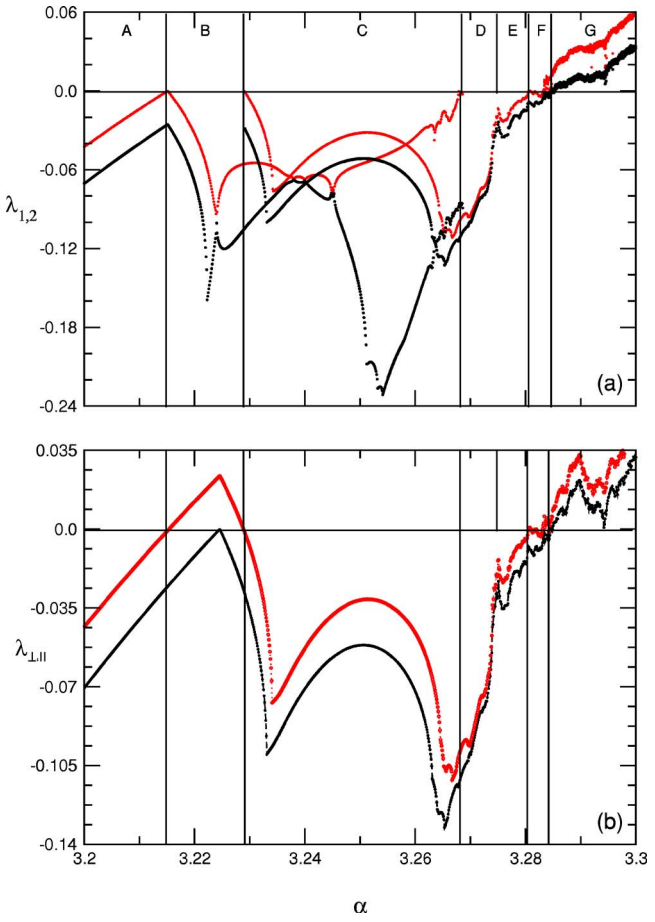

FIG. 2. (Color online) (a) The two largest Lyapunov exponents $\lambda_{1,2}$, and (b) the transverse and in-plane Lyapunov exponents for the invariant subspace, as a function of the parameter α.

region C of Fig. 2, there are two distinct pairs of LEs.

Different bifurcations and transitions can be detected in the variation of the LEs as a function of α. A negative transverse Lyapunov exponent gives stable dynamics in the ISS, and depending on ancillary properties, the dynamics can be either on a synchronous torus, synchronous SNA, or even synchronized chaotic dynamics. The different regimes in Fig. 2(a) are labeled for convenience and we describe the dynamics in detail below.

Prior to the first period-doubling bifurcation at $\alpha \approx 3.2151$, there is a single attractor in the phase space, located in the synchronization manifold (region A). In region B, a nonsynchronous stable torus attractor with two branches outside the ISS coexists with a saddle torus in the ISS. There is another torus-doubling bifurcation of the saddle in the ISS in region B that gives rise to an unstable two branch saddle. The two branch saddle in the ISS becomes stable at $\alpha_c \approx 3.229\,04$ through a subcritical pitchfork bifurcation (region C). The phase portraits in the (x,y) and (θ,x) planes are shown in Fig. 3 for the dynamics in the regions A, B, and C of Fig. 2. In the regions D and E, there are globally stable torus and strange nonchaotic attractors respectively. In region F, the attractor in the ISS is a SNA, while outside the ISS, the attractor is chaotic, while in region G, the attractors both in and outside the ISS are chaotic.

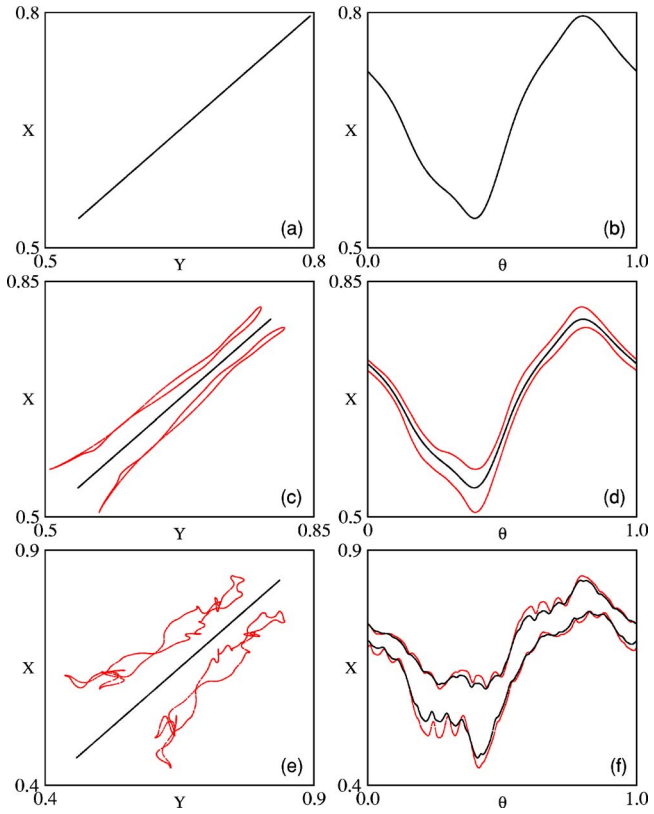

FIG. 3. (Color online) Phase portraits in the (x,y) and (θ,x) planes for dynamics that is synchronized (black) and desynchronized (red), at different values of α. (a)–(b) The synchronous attractor at $\alpha=3.21$ (region A of Fig. 2); (c)–(d) the synchronous and period 2 asynchronous attractors at $\alpha=3.22$ (region B of Fig. 2); (e)–(f) period 2 synchronous and asynchronous attractors at $\alpha=3.25$ (region C of Fig. 2).

These dynamical transitions are naturally accompanied by changes in the attractor basins. In the quasiperiodically forced coupled system, we have symmetric and asymmetric quasiperiodic orbits with two branches. For $\alpha < \alpha_c$, all initial conditions outside the ISS are attracted asymptotically to the nonsynchronous attractors outside the ISS. As the control parameter crosses the critical value $\alpha_c \approx 3.229\,04$, some of the initial conditions (x_0, y_0, θ_0) lie in the basin of the synchronous attractor inside the ISS. The basins of the coexisting attractors in the bistability region are shown in Fig. 4 for different values of α. The relative volume of the basin of the synchronous attractor can be measured as the fraction of initial conditions f that lead to synchronization,

$$f = \frac{N_s}{N_t}, \tag{11}$$

N_s being the number of points converging onto the synchronous attractor in the ISS, out of N_t initial conditions. The dependence of f on α is shown in Fig. 5, the initial value $\theta_i = 0.25$ being fixed.

At the transition to bistability, the basin volume actually increases as a power [32] in the (excess) nonlinearity parameter,

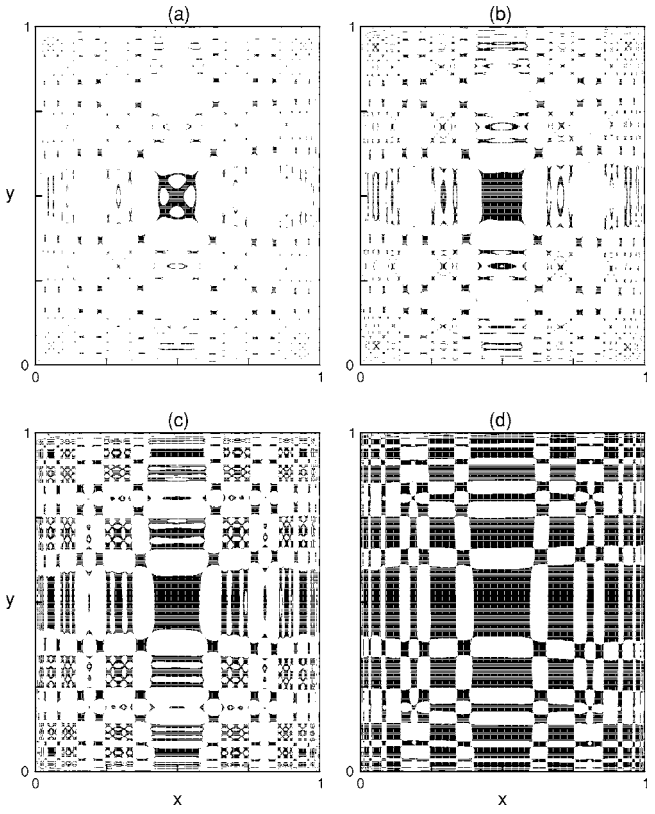

FIG. 4. The basin of attraction of synchronous dynamics (the dark regions) showing the bistable state of the system at (a) $\alpha = 3.229\,04$, (b) $\alpha = 3.2291$, (c) $\alpha = 3.2305$, and (d) $\alpha = 3.2511$.

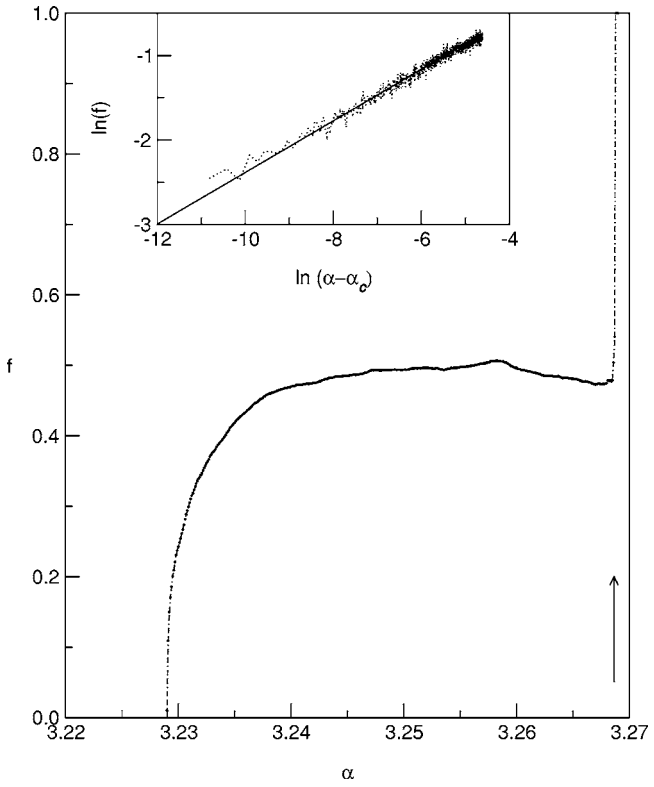

FIG. 5. The crisislike increase in the attractor-basin volume can be gauged by the fraction f of initial conditions that lead to synchronous dynamics as a function of the control parameter α. The inset shows scaling of f vs $(\alpha - \alpha_c)$ with $\alpha_c = 3.229\,04\ldots$. The transition, marked by the arrow, to a single synchronous attractor, occurs at $\alpha \sim 3.2688\ldots$.

$$f \sim (\alpha - \alpha_c)^{\gamma}, \tag{12}$$

as can be seen in the inset of Fig. 5. The scaling exponent γ obtained from numerical simulations is ≈ 0.3, with $\alpha_c \approx 3.229\,04$. It should be noted that the attractors themselves barely change under variation of the parameter. In the case of the unforced coupled map we find the appearance of bistability with a scaling exponent $\gamma \approx 0.13$ for $\beta = 0.01$ and the critical value of α from Eq. (10) as $\alpha_c = 3.010\,074\,62$. The sudden increase in the size of the basin resembles a crisis, although at, for example, an interior crisis [33], this usually pertains to the size of the chaotic attractor itself [34] and not the basin *per se*. Interior crises are also known to occur in quasiperiodic systems [35,36] but with different exponents, suggesting that the mechanisms underlying basin expansion and attractor expansion are probably different. We are presently studying these systems further with a view to understanding these differences [37].

IV. BASIN BIFURCATIONS

The manner in which attractor basins change with parameter have been studied both for a single map, as well as in coupled (but without forcing) maps [38,39]. We combine these two approaches to study the basin bifurcation in the forced coupled system.

Critical manifolds have been an important tool in the study of noninvertible maps [24,40], namely those that are characterized by the fact that a point can possess a different number of preimages, depending on where it is located in the state space. The fundamental role of critical points in one-dimensional noninvertible maps has been extensively studied by several authors, in particular by Gumowski and Mira [41]. For a point y for a given map f in the interval I, a preimage of rank 1 is a point x in I that is mapped to $y : y = f(x)$. One can divide the interval I in zones $z_0, z_1, \ldots$, where z_n is the set of all points having n distinct preimages [24].

Critical points for a noninvertible map thus have at least two preimages, and are those points where the determinant of the Jacobian of the map vanishes. For one-dimensional maps they correspond to local extrema; the present system, for the case $\epsilon = \beta = 0$, reduces to the logistic map and is an example of a z_2 map with critical point $x = 0.5$. For bounded iterated sequences, the iterates of the critical points determine either the boundary of an absorbing region or that of the chaotic attractor [41].

Generalizing this approach to two dimensions yields critical curves instead of points [24,40,42]. Gardini *et al.* [38] have studied a system of two coupled logistic maps and have determined the properties of global bifurcations through a detailed examination of the role of critical curves. Dynamical phenomena such as band merging or interior crises, which have some similarity to phase transitions, can also be understood by examining the dynamics of the critical points in the map [33].

In two-dimensional noninvertible maps, the critical curves are computed as follows. Let $M:R^2 \to R^2$ be a smooth two-dimensional noninvertible map. A rank-1 critical set LC_0 is the set of points having at least two rank-1 preimages on the set LC_{-1}. Hence LC_0 is generally the image of LC_{-1} that is determined by the condition that the determinant of the Jacobian J of M vanishes. The critical curve LC_m is then the rank $-(m+1)$ critical set of $M:LC_m = M^{m+1}(LC_{-1})$, $m=0,1,2,\ldots$.

Feudel *et al.* [43] have generalized these notions to the case of three dimensions. They specifically considered a system of two coupled logistic maps forced by a circle map, and showed that the destruction of tori correlates with the behavior of the iterates of the critical surfaces. In another extension, basin bifurcations in a quasiperiodically forced system, corresponding to the appearance of islands, was also explained via critical curves [39].

Adapting this approach to the present instance, for the three-dimensional map M (Eq. (1)), we obtain critical surfaces instead of critical curves. The rank $-(m+1)$ critical surfaces can be defined as $SC_m = M^{m+1}(SC_{-1})$, $m=0,1,2,\ldots$, and the set SC_{-1} is determined by the following condition for the Jacobian matrix J:

$$\det J(x,y,\theta) = 0. \tag{13}$$

For the map M, the two-dimensional surface SC_{-1} is given by the union of the two surfaces $SC_{-1,a}$ and $SC_{-1,b}$, which both fulfill the condition

$$x = \frac{1}{2} + \frac{\beta(1-2y)}{2\{\alpha[1+\epsilon\cos(2\pi\theta)](2y-1)+\beta\}}, \quad \forall\ \theta. \tag{14}$$

At fixed $\alpha=3.23$ (see arrow BB in Fig. 1) there is a bifurcation in the basin structure as ϵ' increases through a critical value $\epsilon'_c \approx 0.276$. The relative volume of the basin of the ISS attractor, shown in Fig. 6(a) for fixed initial value of $y_i=0.25$, decreases linearly as a function of ϵ' at the basin bifurcation. Since it is difficult to study critical surfaces and basin structure in three dimensions, we fix the variable y at $y_i=0.25$ and study the reduced critical curves in the two-dimensional (x,θ) surface. (These are in fact cross sections of the critical surfaces at the chosen value of y.) In general, a basin bifurcation always results from the contact of a basin boundary with a segment of a critical curve. (See Fig. 6)

The basin of the ISS attractor (in dark) is plotted together with the critical curves in Fig. 7 for different values of the forcing parameter, ϵ'. There are two groups of critical curves that hit the basin boundaries at different control parameter values and give rise to a sequence of three bifurcations that result in the appearance of holes and islands. In Fig. 7(a), we have shown the basin and the critical curves before the first basin bifurcation, for $\epsilon'=0.25$. The first change in the structure of the basin of the ISS attractor takes place at a critical value $\epsilon'_{c1} \approx 0.278$ where white holes in the black basin are created due to a touching of the critical curve LC_3 from the upper set of the critical curves and the basin boundary of the ISS attractor as shown in Fig. 6(b) and Fig. 7(b). The appearance of the holes corresponds to the emergence of initial conditions that converge to the asynchronous attractor within the basin of attraction of the synchronous attractor.

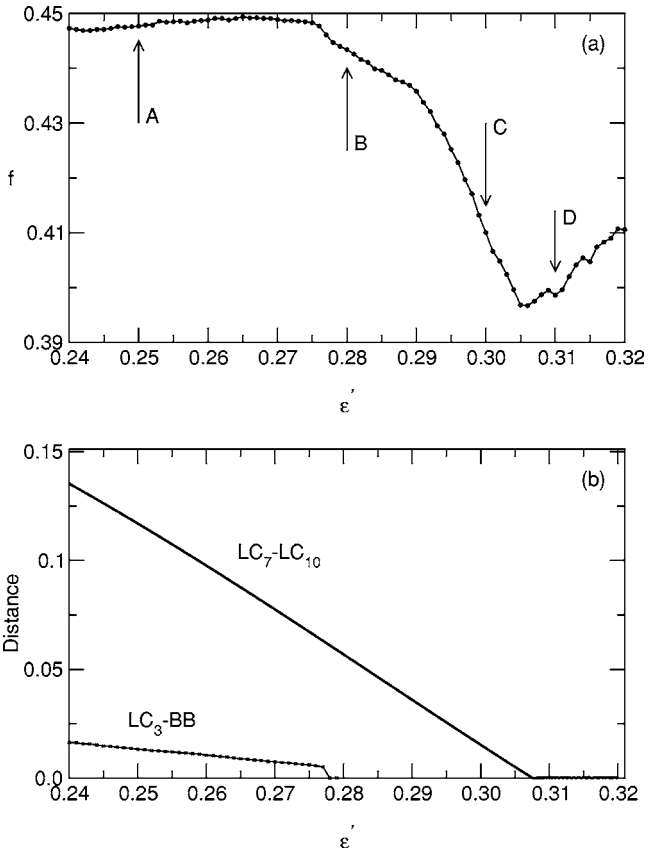

FIG. 6. (a) The fraction of initial conditions f that lead to synchronous dynamics as a function of the control parameter ϵ'. (b) The distance between the basin boundary and the critical curve LC_3 and between the critical curves LC_7 and LC_{10} as a function of the control parameter ϵ' leading to different contact bifurcations.

A second change occurs at a bifurcation related to the appearance of black islands of the ISS attractor basin *within* the white basin of the attractor outside the ISS. This occurs when the lower set of critical curves hits the boundaries of the ISS attractor basin from the outside, as shown in Fig. 7(c). Thus, a portion of the basin of the non-ISS attractor is diverted to the synchronous attractor.

The third modification of the basin structure is due to a sequence of aggregations of islands and a merging of the two bands of the ISS attractor basin, as shown in Fig. 7(d). To estimate the bifurcation point of the merging, the distance between the critical curves LC_7 and LC_{10} from the two branches is calculated as a function of control parameter ϵ'. Figure 6(b) shows the corresponding bifurcation at $\epsilon'_{c3} \approx 0.3076$.

Thus, in all, there are three distinct bifurcations that lead to specific changes in the basin structure. All of these can be identified by examining contact bifurcations of critical surfaces and point to the special role played by critical points and their extensions in multidimensional systems.

V. DISCUSSION AND SUMMARY

In the present work we have examined the case of two identical, symmetrically coupled driven nonlinear systems,

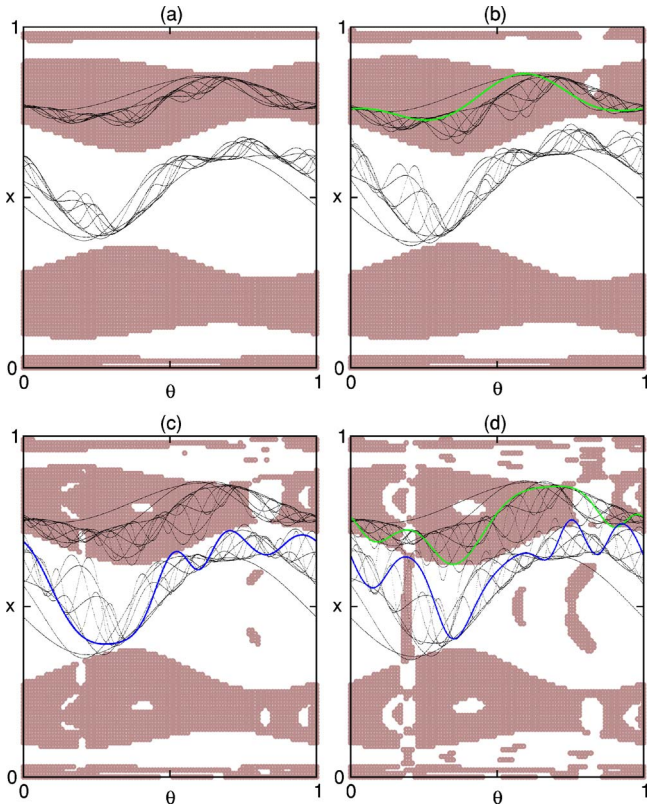

FIG. 7. (Color online) The basin of attraction of synchronous dynamics (dark regions) in the bistable state of the system for $\alpha = 3.23$ at (a) $\epsilon' = 0.25$ (arrow A in Fig. 6(a)), (b) $\epsilon' = 0.28$ (arrow B in Fig. 6(a)), (c) $\epsilon' = 0.30$ (arrow C in Fig. 6(a)), and (d) $\epsilon' = 0.31$ (arrow D in Fig. 6(a)). The critical curves LC_3 in (b) are prominently marked green and LC_8 in (c) is marked blue, and LC_7 and LC_{10} in (d) are green and blue, respectively.

namely coupled logistic maps with multiplicative quasiperiodic forcing. We have studied a limited but representative region in parameter space, and seen that this system has a rich variety of dynamics: quasiperiodic (torus) dynamics, strange nonchaotic, and chaotic motion. Furthermore, the two systems can be synchronized or desynchronized, and can have multiple coexisting attractors, namely bistability or multistability.

A novel phenomenon observed at the onset of bistability is the power-law growth of the volume of the basin of the synchronous attractor. Although superficially similar to an interior crisis [23] when the attractor volume increases according to a power law, here the attractors do not change significantly while their basins expand. Further, while it is clear that the competing basins are interpenetrating, often the basin boundaries are themselves smooth. It may be possible to use the framework of interior crises to explain this phenomenon when the basin boundaries are fractal and contain embedded chaotic saddles [37].

Basin bifurcations in the bistability region are explained via the concept of critical surfaces. After the first contact bifurcation, holes appear in the basin of the ISS attractor and correspond to points that converge to the other (asynchronous) attractor. As the control parameter increases, there is a creation of islands of points that go to the ISS attractor in the basin of the other asynchronous attractor. As the number of islands increase, the two bands of the ISS attractor basin merge at a critical value of the control parameter. These three bifurcations lead to characteristic changes in the structure of the basins of attraction.

The initial explorations of coupled driven systems presented here need to be extended in a number of different directions. The distinct regimes of synchronization suggest that quasiperiodic driving could be used as a method for control [44]. The implications of coupling a large number of systems (on a coupled map lattice, for instance) and driving them individually or collectively have not been studied in any detail so far [45], and it can be anticipated that there will be a wealth of new phenomena to uncover.

ACKNOWLEDGMENTS

This research was supported by Department of Science and Technology, India, and by the DAAD- DST exchange program.

[1] K. Kaneko, *Theory and Applications of Coupled Map Lattices* (Wiley, New York, 1993).
[2] K. Kaneko, Prog. Theor. Phys. **72**, 480 (1984); Chaos **2**, 279 (1992); and references therein.
[3] L. Glass and M. C. Mackey, *From Clocks to Chaos: The Rhythms of Life* (Princeton University Press, Princeton, 1988).
[4] M. C. Cross and P. C. Hohenberg, Rev. Mod. Phys. **65**, 851 (1993).
[5] A. Prasad, S. S. Negi, and R. Ramaswamy, Int. J. Bifurcation Chaos Appl. Sci. Eng. **11**, 291 (2001), and references therein.
[6] A. Prasad and R. Ramaswamy, Phys. Rev. E **60**, 2761 (1999); see also *Nonlinear Dynamics: Integrability and Chaos*, edited by M. Daniel, R. Sahadevan, and K. Tamizhmani (Narosa, New Delhi, 1998), p. 227.
[7] Y. C. Lai, C. Grebogi, J. A. Yorke, and S. C. Venkataramani, Phys. Rev. Lett. **77**, 55 (1996).
[8] V. Astakhov, A. Shabunin, T. Kapitaniak, and V. Anishchenko, Phys. Rev. Lett. **79**, 1014 (1997); Y. L. Maistrenko, V. L. Maistrenko, A. Popovich, and E. Mosekilde, Phys. Rev. E **57**, 2713 (1998); **60**, 2817 (1999).
[9] C. Grebogi, E. Ott, S. Pelikan, and J. A. Yorke, Physica D **13**, 261 (1984).
[10] J. F. Heagy and S. M. Hammel, Physica D **70**, 140 (1994).
[11] K. Kaneko, Prog. Theor. Phys. **71**, 1112 (1984).
[12] S. Kuznetsov, U. Feudel, and A. Pikovsky, Phys. Rev. E **57**, 1585 (1998).
[13] A. Pikovsky, M. Rosenblum, and J. Kurths, *Synchronization: A Universal Concept in Nonlinear Science* (Cambridge University Press, Cambridge, 2001).
[14] L. M. Pecora and T. L. Carroll, Phys. Rev. Lett. **64**, 821

(1990).
[15] J. F. Heagy, T. L. Carroll, and L. M. Pecora, Phys. Rev. E **50**, 1874 (1994); K. Josic, Phys. Rev. Lett. **80**, 3053 (1998).
[16] H. Fujisaka and T. Yamada, Prog. Theor. Phys. **69**, 32 (1983).
[17] R. Ramaswamy, Phys. Rev. E **56**, 7294 (1997).
[18] E. Neumann, I. Sushko, Y. Maistrenko, and U. Feudel, Phys. Rev. E **67**, 026202 (2003).
[19] T. E. Vadivasova, O. V. Sosnovtseva, A. G. Balanov, and V. V. Astakhov, Phys. Rev. E **61**, 4618 (2000).
[20] U. Feudel, C. Grebogi, B. R. Hunt, and J. A. Yorke, Phys. Rev. E **54**, 71 (1996).
[21] U. Feudel and C. Grebogi, Chaos **7**, 597 (1997).
[22] U. Feudel and C. Grebogi, Phys. Rev. Lett. **91**, 134102 (2003).
[23] C. Grebogi, E. Ott, and J. A. Yorke, Phys. Rev. Lett. **48**, 1507 (1982).
[24] C. Mira, L. Gardini, A. Barugola, and J. C. Cathala, *Chaotic Dynamics in Two-Dimensional Noninvertible Maps* (World Scientific, Singapore, 1996).
[25] J. Milnor, Commun. Math. Phys. **99**, 177 (1985).
[26] E. Ott and J. C. Sommerer, Phys. Lett. A **188**, 39 (1994).
[27] E. Ott, *Chaos in Dynamical Systems* (Cambridge University Press, Cambridge, 2002).
[28] A. V. Taborov, Yu. L. Maistrenko, and E. Mosekilde, Int. J. Bifurcation Chaos Appl. Sci. Eng. **10**, 1051 (2000).
[29] V. Astakhov, A. Shabunin, W. Uhm, and S. Kim, Phys. Rev. E **63**, 056212 (2001).
[30] C. Reick and E. Mosekilde, Phys. Rev. E **52**, 1418 (1995).
[31] B. P. Bezruchko, M. D. Prokhorov, and Ye. P. Seleznev, Chaos, Solitons Fractals **15**, 695 (2003).
[32] A. G. Siapas, Phys. Rev. Lett. **73**, 2184 (1994).
[33] C. Grebogi, E. Ott, and J. A. Yorke, Phys. Rev. Lett. **48**, 1507 (1982); Physica D **7**, 181 (1983).
[34] V. Mehra and R. Ramaswamy, Phys. Rev. E **53**, 3420 (1996).
[35] A. Prasad, V. Mehra, and R. Ramaswamy, Phys. Rev. Lett. **79**, 4127 (1997).
[36] A. Witt, U. Feudel, and A. S. Pikovsky, Physica D **109**, 180 (1997).
[37] M. D. Shrimali, A. Prasad, R. Ramaswamy, and U. Feudel, in preparation.
[38] L. Gardini, R. Abraham, R. J. Record, and D. Fournier-Prunaret, Int. J. Bifurcation Chaos Appl. Sci. Eng. **4**, 145 (1994).
[39] U. Feudel, A. Witt, Y. C. Lai, and C. Grebogi, Phys. Rev. E **58**, 3060 (1998).
[40] C. Mira, D. Fournier-Prunaret, L. Gardini, H. Kawakami, and J. C. Cathala, Int. J. Bifurcation Chaos Appl. Sci. Eng. **4**, 343 (1994).
[41] I. Gumowski and C. Mira, *Recurrences and Discrete Dynamical Systems* (Springer-Verlag, Berlin, 1980).
[42] C. Mira, Nonlinear Anal. Theory, Methods Appl. **4**, 1167 (1980).
[43] U. Feudel, M. A. Safonova, J. Kurths, and V. S. Anishchenko, Int. J. Bifurcation Chaos Appl. Sci. Eng. **6**, 1319 (1996).
[44] G. Hu, J. Xiao, J. Yang, F. Xie, and Z. Qu, Phys. Rev. E **56**, 2738 (1997); S. Boccaletti, J. Bragard, and F. T. Arecchi, *ibid.* **59**, 6574 (1999).
[45] O. Sosnovtseva, T. E. Vadivasova, and V. S. Anishchenko, Phys. Rev. E **57**, 282 (1998).